Identification of target actin content and polymerization status as a mechanism of tumor resistance after cytolytic T lymphocyte pressure

Soraya Abouzahr*, Georges Bismuth†, Catherine Gaudin*, Oliver Caroll‡, Peter Van Endert‡, Abdelali Jalil*, Jean Dausset§¶, Isabelle Vergnon*, Catherine Richon*, Audrey Kauffmann‖, Jérôme Galon**, Graca Raposo††, Fathia Mami-Chouaib*, and Salem Chouaib*¶

*Institut Gustave Roussy, Institut National de la Santé et de la Recherche Médicale U487, 94805 Villejuif, France; †Institut Cochin, Institut National de la Santé et de la Recherche Médicale U567, Centre National de la Recherche Scientifique, Unité Mixte de Recherche 8104, Université René Descartes, 75014 Paris, France; ‡Institut National de la Santé et de la Recherche Médicale U580, Université René Descartes, 75015 Paris, France; ††Institut Curie Research Section, Centre National de la Recherche Scientifique, Unité Mixte de Recherche 144, 75248 Paris Cedex 5, France; **Centre de Recherches Biomédicales des Cordeliers, Institut National de la Santé et de la Recherche Médicale U255, 75006 Paris, France; ‖Institut Gustave Roussy, Centre National de la Recherche Scientifique, Unité Mixte de Recherche 8125, 94805 Villejuif, France; and §Centre d'Etude du Polymorphisme Humain, 75010 Paris, France

Contributed by Jean Dausset, December 7, 2005

To investigate tumor resistance to T cell lysis, a resistant variant was selected after specific cytolytic T lymphocytes (CTL) selection pressure. Although the resistant variant triggered *perforin* and *granzyme B* transcription in specific CTLs, as well as their degranulation, it exhibited a dramatic resistance to cytotoxic T cell killing. It also displayed strong morphological changes with alterations of the actin cytoskeleton. Electron microscopy analysis revealed a loosen interaction between CTLs and the resistant variant despite the formation of apparently normal conjugates. Transcriptional profiling identified a gene expression signature that distinguished sensitive from resistant tumor targets. More notably, we found that actin-related genes *ephrin-A1* and *scinderin* were overexpressed in resistant target. Silencing of these genes using RNA interference resulted in a restoration of normal cell morphology and a significant attenuation of variant resistance to CTL killing. Our present study shows that a shift in cytoskeletal organization can be used, by tumor cells, as a strategy to promote their resistance after CTL selection pressure.

cell-mediated cytotoxicity | ephrin-A1 | scinderin

CD8+ cytolytic T lymphocytes (CTL) are important effector cells during tumor rejection. This view is supported by a number of experimental (1) and clinical data (2). Currently, most attempts at cancer immunotherapy involve the generation of CTLs against tumor-associated antigens (TAA). The identification of these antigens and their T cell epitopes recognized by autologous T cells has led to their broad use as immunogens to induce or augment TAA-specific immune responses in vaccination strategies. However, the understanding of tumor–host interactions remains elusive despite this identification. In this respect, tumor rejection in patients does not always follow successful induction of tumor-specific immune responses by cancer vaccine immunotherapy. Evidence has been provided indicating a paradoxical coexistence of cancer cells with TAA-specific immune cells in tumor-competent host. There are increasing indications that tumor cells play a crucial role in the control of immune protection (3) and contain many overlapping mechanisms to maintain their functional disorder and evasion. Furthermore it has been reported by Dunn *et al.*, that tumor specific T cell responses may prevent tumor cell growth, but they may also select for tumor antigen negative and resistant variants *in vivo* (4, 5). It is likely that tumor escape variants will emerge most frequently in the context of effective immunotherapies (6). Clearly, even if a strong and sustained cytotoxic response is induced, complex issues such as tumor evasion and selection of tumor-resistant variants remain.

Even though resistance of tumor cells to cell-mediated cytotoxicity remains a drawback in the immunotherapy of cancer, its molecular basis is poorly understood. A great deal of effort has been focused on trying to understand the tumor escape to immune surveillance and to understand the molecular basis of tumor tolerance (7, 8). However, a comprehensive analysis of gene regulation has not yet been performed although several pathways and genes were associated with tumor resistance to CTL killing (9, 10).

Various studies on actin-associated protein demonstrate that changes in the expression of specific structural component of the actin cytoskeleton can contribute to tumorigenesis (11). Recently, it has been shown that morphological change of tumor cells may affect their susceptibility to cytotoxic treatments (12), and that the cytoskeleton plays a critical role in various cellular processes, linked to regulation of apoptosis (13), natural killer (NK)-mediated lysis (14), and T cell activation (15, 16). However, little is known about the consequence of morphological change of target cells on CTL-mediated cytotoxicity. In this regard, the cytoskeleton can no longer be considered only as structural framework playing a role in cell shape adhesion, motility, exocytosis, and endocytosis. Clearly, actin dynamics that are regulated by a complex interplay of the small GTPase proteins of Ras superfamily Rac, Rho, and Cdc42 (17), coordinate multiple signaling pathways including effector/target relation through their ability to regulate both the cytoskeleton and transcription of specific target genes. In the present studies, we analyzed the gene expression profile associated with the acquisition of tumor resistance to specific lysis. For this purpose, we used a microarray analysis in combination with online PCR. The results of the present study indicate that morphological change due to overexpression of *scinderin* and *ephrin-A1* resulted in alteration of actin polymerization and content that might act as a molecular switch in the control of tumor target susceptibility to CTL killing.

Results

***In Vitro* CTL Selection Pressure Induces the Selection of Tumor-Resistant Variants to Specific Lysis.** For this study, we used a human non-small-cell lung carcinoma cell line IGR-Heu and the autologous CTL clone Heu161 (CD3+, CD8+, CD4−, and CD28−). Heu161 displays a strong cytotoxic activity against IGR-Heu au-

Conflict of interest statement: No conflicts declared.

Abbreviations: CTL, cytolytic T lymphocytes; TAA, tumor-associated antigen; siRNA, small interference RNA.

Data deposition: The microarray data related to this paper have been submitted to the Array Express data repository at the European Bioinformatics Institute, www.ebi.ac.uk/arrayexpress (accession no. E-TABM-71).

¶To whom correspondence may be addressed. E-mail: chouaib@igr.fr or dausset@cephb.fr.

www.pnas.org/cgi/doi/10.1073/pnas.0510454103

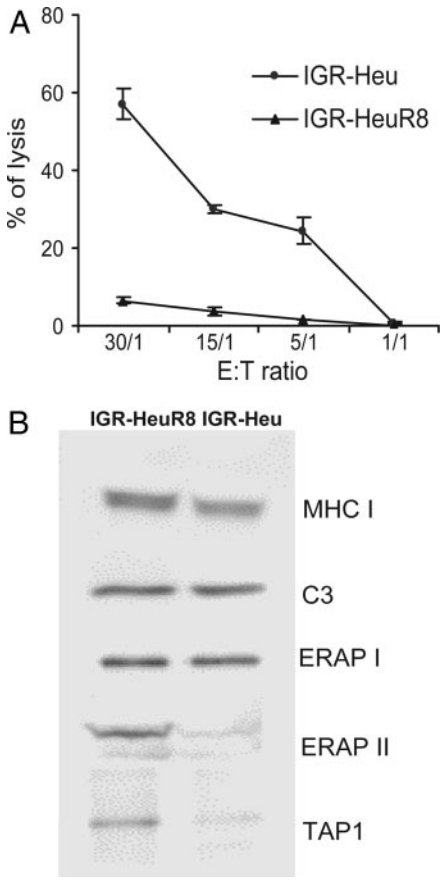

Fig. 1. Phenotypical and functional characterization of the IGR-HeuR8-resistant clone. (*A*) Cytotoxic activity of Heu161 on IGR-Heu autologous large-cell carcinoma cell line and the selected clone IGR-HeuR8. Cytotoxicity was determined by a conventional 4-h ^{51}Cr release assay at the indicated effector/target ratios. Data shown are representative of three independent experiments. (*B*) Analysis of MHC class I, TAP, and ERAP expression. ERAPI, MHC class I, and TAP-1 were analyzed by immunoprecipitation followed by immunblotting. ERAP1 was detected with mAb 6H9 and MHC class I with a rabbit polyclonal antibody. TAP-1 was detected with mAb 148.3. Proteasome was detected by using mAb MCP21.

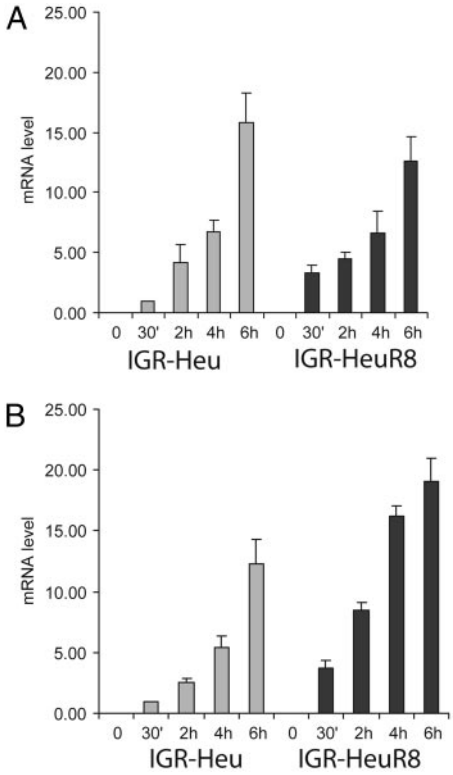

Fig. 2. Transcription and secretion of lytic granules by Heu161 CTL upon stimulation with the sensitive cell line and the derived resistant variant. Expression of *granzyme B* (*A*) and *perforin* (*B*) genes in CTL Heu161 after stimulation with the sensitive IGR-Heu cell line or with the resistant IGR-HeuR8 cell clone. Quantitative real-time PCR analysis of RNA isolated from conjugate left for the indicated time (0, 30 min, 2 h, 4 h, and 6 h) was performed as described in *Experimental Procedures.* Data are representative of three individual experiments.

tologous tumor cell line (18). After sustained coculture of tumor cells with Heu161, a resistant variant line, IGR-HeuR, was established. Using limiting dilution, several resistant variant clones were isolated. Among these resistant variants, IGR-HeuR8 was selected for further studies on the basis of its conserved antigen-encoding gene expression (data not shown) and resistance to CTL killing even at high effector/target ratio (Fig. 1*A*).

Resistance to killing by CTL can be caused by impaired cellular antigen processing and/or presentation. To address this issue, we studied the expression levels of several proteins involved in antigen processing and presentation by HLA class I molecules. Immunoblot analysis (Fig. 1*B*) revealed equivalent expression levels of the constitutive proteasome subunit C3, of MHC class I heavy chains and of the endoplasmic reticulum (ER) aminopeptidase ERAP1. Expression of the TAP1 peptide transporter subunit and the second ER peptidase ERAP2 was increased in the resistant cells. Thus, impaired antigen processing, as a cause for the resistance of IGR-HeuR8 cells to CTL lysis, is unlikely. In addition, immunofluorescence analysis shows that the expression of MHC class I molecules HLA-A/B/C, HLA B/C, HLA-A2, adhesion molecules ICAM-1, LFA3, and the costimulatory molecule CD86 were similarly expressed by the resistant variant (IGR-HeuR8) and the parental line (IGR-Heu) (data not shown).

The Tumor-Resistant Variant Efficiently Induces *granzyme B* and *perforin* Transcription as Well as Degranulation of the Specific CTL Clone. We have previously shown that IGR-Heu cells were defective for Fas/CD95, TRAIL-R1/DR4, TRAIL-R2/DR5, and TNF-R1 death receptor surface expression and that autologous CTL mainly used the secretory pathway to lyse specific target cells (19). To investigate the stimulatory potential of the resistant variant, the Heu161 CTL clone was incubated in the presence of either the IGR-Heu parental cell line or the IGR-Heu-R8-resistant variant. Quantitative PCR analysis demonstrated that stimulation of the CTL clone by sensitive and resistant targets resulted in a significant and similar transcription levels of *granzyme B* (Fig. 2*A*). Strikingly, a more pronounced transcription of *perforin* gene was observed when the CTL clone was stimulated with the resistant variant (Fig. 2*B*). It is also interesting to note that the stimulation of the CTL clone by the parental cell line and the resistant variant induced cytotoxic molecule degranulation as revealed by CD107 induction on the CTL clone surface (data not shown).

Electron Microscopy Analysis of the Conjugates Formed Between CTLs and Resistant Tumor Cells Reveals a Loosen Synapse. Despite the comparable number and the apparent stability of conjugates formed between tumor cells and autologous CTL (data not shown), alteration of the synapse between CTLs and resistant tumor cells may occur. We thus further evaluated synapse

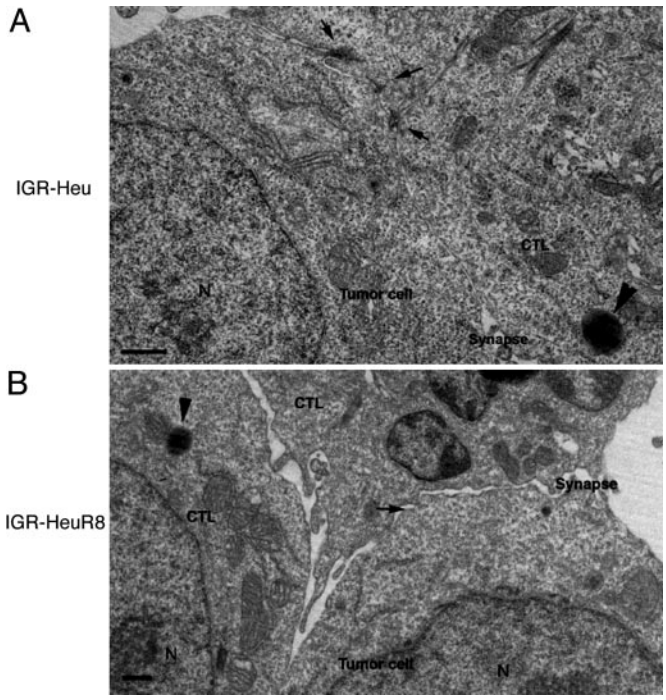

Fig. 3. Electron microscopic analysis of ultrathin sections of CTL-sensitive and -resistant tumor cell conjugates. (*A*) After 15 min of contact, very close contacts are observed between the sensitive target and the CTL (see arrows for examples). Note the electron-dense filaments accumulated at the contact points. (*B*) Resistant targets are observed in close proximity to the CTLs, but contact between points is not very close. Arrowheads: lytic granule N (nucleus). (Scale bars, 200 nm.)

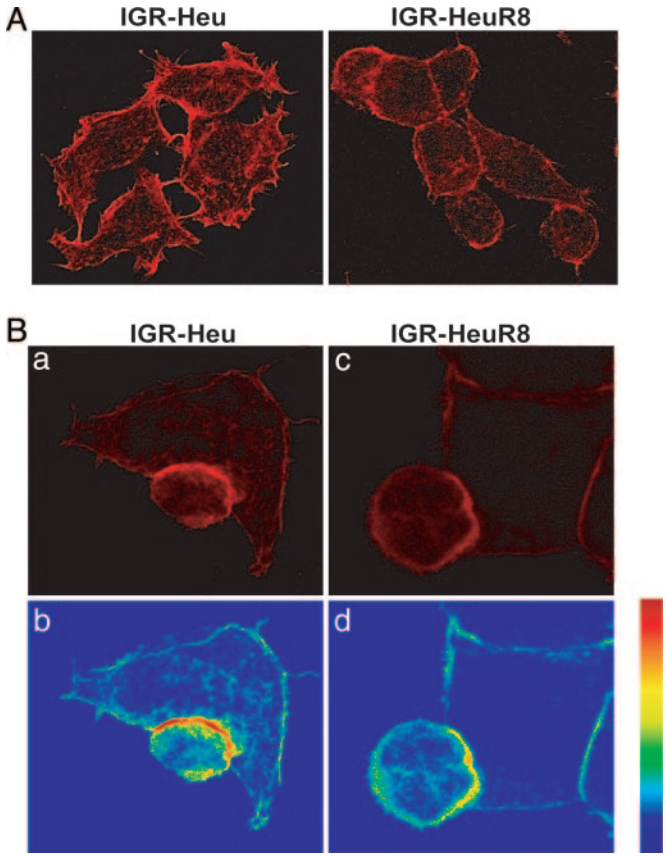

Fig. 4. Analysis of the morphology of resistant variant and conjugate formation with autologous CTL. (*A*) Microscopic analysis of cell morphology. IGR-Heu and IGR-HeuR8 were plated on glass coverslips and stained with 568 Alexa Fluor–phalloidin before analysis with a Zeiss Axiovert 200 inverted fluorescence microscope. Data are from one representative experiment of at least three. (*B*) Microscopic analysis of synaptic polymerized actin. Tumor cells were incubated with autologous CTL for 30 min at 2:1 ratio. After washing to eliminate nonadherent lymphocytes, conjugates were stained with 568 Alexa Fluor–phalloidin and analyzed with a Zeiss Axiovert 200 inverted fluorescence microscope. *a* and *c*, true color; *b* and *d*, staining intensity (blue to red, low to high). Data are from one representative experiment of at least three for each image.

formation using electron microscopy. As shown in the Fig. 3*A*, very close membrane appositions were observed between the CTL clone and the sensitive target, suggesting a very tight interaction. Interestingly, the accumulation of cytoskeletal filaments was evident at these sites of tight apposition (arrows). In contrast, the synapses formed between CTLs and resistant targets appeared much looser with only occasional tight contacts in the synaptic cleft (Fig. 3*B*). Because CTL-mediated cytotoxicity requires a tight adhesion to the target cell, providing a covered microenvironment for the release of cytotoxic granules, the loosen synapse formed with the tumor cell variant may therefore explain its resistance to CTL killing.

The Acquisition of Resistance Involves Target Cell Morphological Change. Data depicted in Fig. 4*A* show that the acquisition of resistance induced morphological changes in target cells. Indeed, the resistant variant cells acquired a round morphology, with a dramatic reduction of the cells extensions present in the sensitive parental cell line. This was associated with a marked decrease in filamentous actin cellular content, as revealed by Alexa Fluor 568-phalloidin staining, and despite a similar cell size as the sensitive cell line (data not shown). Importantly, actin polymerization at the CTL/resistant target cell synaptic contact was also strongly reduced, as shown in Fig. 4 *Bc* and *d*. This finding indicates that the resistant variant displays a disorganized actin cytoskeleton, and that the acquisition of resistance to CTL-mediated killing might result from a shift in the level of actin polymerization. To further examine this hypothesis, sensitive target cells were treated with latrunculin A, an inhibitor of actin polymerization (20). Such treatment dramatically inhibited its killing by the CTL clone (data not shown). Moreover, when sensitive cells were incubated with latrunculin A, the level of polymerized actin, as well as their morphology, was comparable to that observed in resistant IGR-HeuR8 (data not shown). These results further support that actin organization is a crucial determinant in the control of target susceptibility to CTL and, accordingly, that changes of the actin cytoskeleton may help tumor cells to escape destruction by CTLs.

Ephrin-A1 and Scinderin Overexpression Is Associated with Resistant Variant Morphological Change and Altered Susceptibility to CTL Lysis. To gain further insight into the molecular mechanisms underlying tumor resistance to specific CTL-mediated cytotoxicity, we have conducted a comprehensive microarray analysis using an Agilent 44,000 human oligo microarray. Comparative analysis identified an expression profile of 676 genes that best distinguished resistant variant from parental sensitive target. Functional analysis of transcript profiles identified clusters of genes that were differentially expressed in resistant variant, including a cluster of metabolism, cellular physiological process, cell communication, death, growth, and morphogenesis (data not shown).

To determine the relationship between morphological change, resistance to CTL and gene expression profile, we focused on actin-related genes. As depicted in Table 1, two of the most

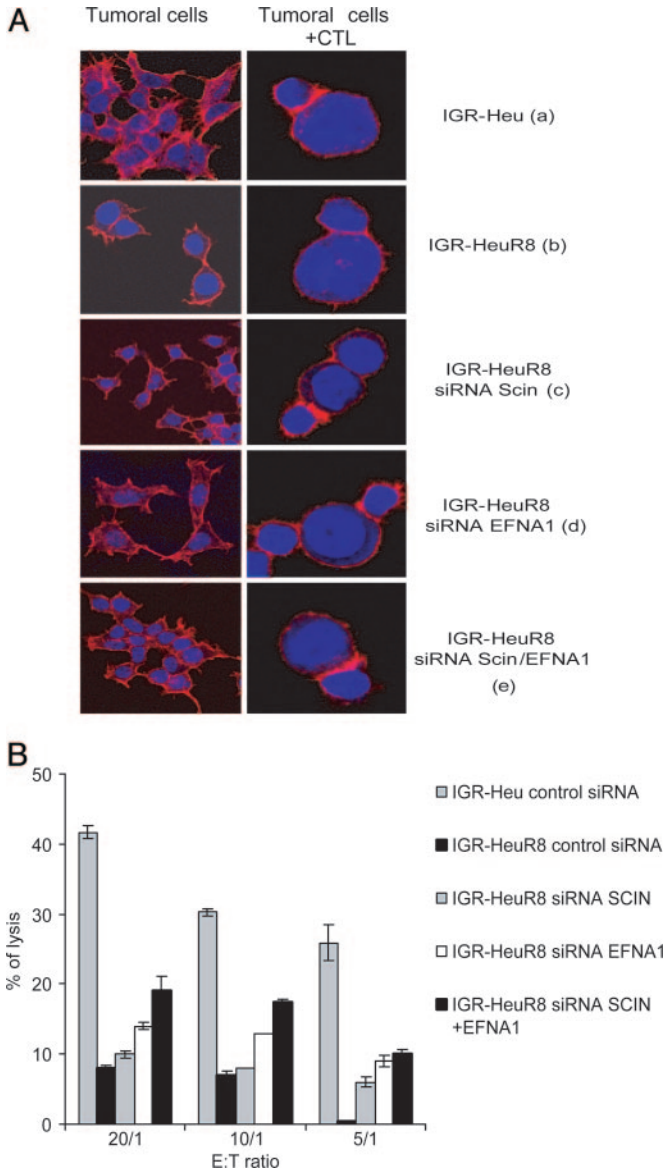

Fig. 5. Morphological and functional consequences of targeting *scinderin* and ephrinA1. (*A*) IGR-HeuR8 clones were transfected with control or siRNA targeting *scinderin* or *ephrin-A1* or a combination of both. Seventy-two hours after transfection, IGR-HeuR8 were incubated with the CTL. The conjugates were bound to poly(L-lysine)-treated coverslips, fixed, and stained with 568 Alexa Fluor–phalloidin for visualization of polymerized filamentous actin (red). Data are from one representative experiment of three. (*B*) Killing of IGR-HeuR8 by autologous CTL after inhibition of *scinderin* and *ephrin-A1* or the combination of both. ^{51}Cr-labeled cells were incubated at 37°C with CTL at different ratios. After 4 h, the supernatants were collected and analyzed by γ counter. The results obtained are statistically relevant.

consistently relevant genes, overexpressed in resistant cells, were *ephrin-A1* and *scinderin*. Scinderin is involved in the control of dynamic changes of actin cytoskeleton networks (21), and ephrin-A1, a glycosylphosphatidylinositol-anchored ligand, has been reported to play a role in the regulation of cytoskeleton organization (22). Importantly, both genes are known to be involved in the control of tumor growth and survival (23–25). Quantitative RT-PCR results confirmed the direction and magnitude of these gene expression changes. *Ephrin-A1* and *scinderin* increased 45.6- and 29.5-fold, respectively, in the resistant variant as compared with the parental target (data not shown).

Table 1. Actin-binding-related genes differentially expressed in resistant and sensitive cell lines

Accession no.	Gene	Fold change	*P* value
NM_033128	*SCIN*	−5.95	8.28×10^{-21}
NM_004428	*EFNA1*	−5.39	0
NM_016445	*PLEK2*	−4.42	0
NM_016341	*PLCE1*	−3.48	1.52×10^{-21}
NM_003633	*ENC1*	−2.94	3.40×10^{-38}
NM_006393	*NEBL*	−2.18	4.63×10^{-21}
A_32_P187875	*CTNNB1*	−2.03	1.48×10^{-26}
NM_004415	*DSP*	−2.00	0
NM_033138	*CALD1*	2.05	0
NM_004543	*NEB*	2.11	0
NM_003290	*TMP4*	2.14	2.03×10^{-14}
NM_000109	*DMD*	2.35	0
NM_012307	*EPB41L3*	2.48	0
BX647344	*AVIL*	3.34	1.10×10^{-15}
NM_006175	*NRAP*	3.53	6.25×10^{-35}
NM_001839	*CNN3*	4.17	2.19×10^{-43}

RNA Interference-Mediated Silencing of *scinderin* and *ephrin-A1* Genes Reverts Resistant Cell Morphology and Increases Their Susceptibility to CTL Killing. To further assess the putative role of *scinderin* and *ephrin-A1* in the control of tumor variant morphology and susceptibility to CTL-mediated killing, transfection of resistant cells IGR-HeuR8 with small interference RNAs (siRNAs) targeting these genes was performed. A specific and efficient reduction of the levels of *ephrin-A1* and *scinderin* protein by 90%, as compared with a control siRNA, was observed 72 h after treatment. Simultaneous knockdown of these genes in the resistant target was accompanied by a striking change in the cell morphology induced upon acquisition of resistance to CTL killing (Fig. 5*Ae*). As shown, the acquisition of resistance-induced cell rounding was reversible. In addition, phalloidin staining revealed an increase in the cellular filamentous actin content and actin polymerization at the synaptic contact of siRNA treated cells as compared with the control resistant target (Fig. 5*Ab*). More importantly, whereas individual knockdown of *scinderin* and *ephrin-A1* resulted in a marginal attenuation of resistance, the simultaneous silencing of both genes significantly increases the sensitivity of the resistant target to CTL killing.

Discussion

The coexistence in cancer patients of tumor cells and tumor-specific circulating CD8+ T cells remains an intriguing paradox of tumor immunology (26, 27). Our present results provide further evidence for the concept of immune selection in neoplastic development by showing that CTL selection pressure can lead to a striking adaptation of the tumor target, involving morphological change to escape immune surveillance. Although the mechanisms by which CTL selection pressure contributes to morphological changes remain to be fully elucidated, it has been recently reported that cytokines, including TNF, can induce actin depolymerization and morphological changes through activation of ERK and orp38 mitogen-activated protein kinase (28).

Despite our increasing knowledge about tumor escape mechanisms, a systematic analysis of tumor resistance to CTL killing has not yet been reported. The present study demonstrates that, after CTL selection pressure, tumor cells acquire resistance to CTL-mediated killing, further outlining that tumor escape variants might emerge most frequently as a result of effective immunotherapies. Several reports support the concept of TAA loss as a potential mechanism to escape immunotherapeutical-induced antitumor response. However, our studies confirm that

the escape of resistant variants to CTL may be also independent of TAA loss (29, 30). We found in this context that T cell recognition did occur, as revealed by T cell reactivation, including granzyme B, perforin transcription, and exocytosis. This emphasizes that T cell reactivation and degranulation are not necessarily associated with the induction of target cell killing. This also suggests that visualization and quantification of antigen-specific T cells should be used in combination with functional assays to distinguish functional heterogeneity between reactive CD8+ T cells and also to assess their therapeutic potential.

It is well known that secretion of cytolytic granule content at the immunological synapse is a highly regulated process that requires the rapid transfer of lytic granules to the target cell interface, followed by their docking and fusion with the plasma membrane. Here, we show that tumor variant resistance does not involve an absence of synapse formation or a defective degranulation of cytotoxic molecules but is associated with an abnormal CTL/target cell interaction, as revealed by electron microscopy analysis. Indeed, the synapses formed between CTLs and resistant targets appeared clearly much looser, with only occasional tight contacts at the CTL–tumor cell interface.

Of particular significance was the demonstration in this study that the acquisition of resistance resulted in a remarkable change in cell morphology as compared with control sensitive cells. This was accompanied by an alteration in actin polymerization, a phenomenon that might act as a molecular switch in the control of tumor susceptibility to CTL killing. In this regard, a correlation between actin levels, the state of its polymerization, and the invasiveness of tumor cells has been reported (31). Studies, focused on the investigation of the occurrence and significance of this morphological change *in vivo* and its contribution to immune selection and emergence of aggressive tumor variants, will also be necessary to know whether our findings are relevant for patients after vaccine or adoptive transfer of effector T cells.

It is well established that actin cytoskeleton plays a crucial role in the regulation of cell signaling (32) and apoptosis (33). Here, we show that *scinderin* and *ephrin-A1*, which play a major role in the control of cytoskeletal organization, were overexpressed in the resistant variant. Ephrins have been shown to be up-regulated in tumors, especially in the more aggressive stages of tumor progression (34) regulating cell attachment, shape, and mobility. Several reports indicate that ephrin receptors, the largest subfamily of receptor tyrosine kinases, and their ephrin ligands are important mediators of cell–cell communication.

The most important finding of our study is that the cytoskeleton organization may impact tumor susceptibility to CTL-mediated lysis. This suggests that changes in cell plasticity after cytoskeletal disorganization is important for the interaction of CTLs with specific target cells and interfere with their killing. This is consistent with the inhibitory effect on CTL-induced cell death of latrunculin A, a specific inhibitor of actin polymerization. Thus, susceptibility to CTL-induced killing requires polymerized actin structures in the target cell to control the formation of an efficient lytic synapse. The involvement of *ephrin-A1* and *scinderin* in the control of cell morphology and susceptibility of resistant variants to CTL was further supported by the inhibitory effect of small siRNA targeting both genes. It is important to point out that such targeting not only reverted cell morphology and filamentous actin content but also partially restored the susceptibility of tumor variant to CTL-induced lysis. However, given that the differential gene expression between sensitive and resistant tumor variants is not restricted only to genes involved in morphogenesis and that gene silencing of *scinderin* and *ephrin-A1* has a partial effect in restoring cell susceptibility to lysis, it is likely that mechanisms other than actin-dependent processes could contribute to tumor cell resistance. These findings also indicate that the cytoskeleton could be a good target to improve tumor lysis, because its alteration under CTL selection pressure can be reversed. It remains, therefore, to be determined how the pathways linked to ephrin-A1 and scinderin, which emerge as important regulators of cell survival and apoptosis, interact with the signaling molecules that play a fundamental role in cytoskeleton reorganization (35).

The work reported here shows that CTL selection pressure induces resistant variants with altered cytoskeleton organization. Our data identify a mechanism by which tumor cells, through actin reorganization, including at the immunological synapse, may regulate CTL reactivity and impede their cytotoxic activity. Thus, it is reasonable to imagine that tumors frequently develop this kind of specific strategy based on cytoskeleton alterations and subsequent changes of cell plasticity to shift the balance from immune surveillance to tolerance. Our findings also confirm that the CTL is only one among many others players of the antitumor response, and that understanding the tumor behavior and its interplay with the effector cells will be a key determinant in a rational approach to tumor immunotherapy. The various strategies aimed at the induction of antitumor cytotoxic responses should therefore consider the morphological change described in this report as an antitumor mechanism of tumor escape, partly involved in resistance of tumor cells to cytotoxicity, despite tumor immunogenicity and CTL reactivity.

Experimental Procedures

Tumor Cell Lines and CTL Clone. The non-small-cell lung carcinoma tumor cell line, IGR-Heu, was derived from a large-cell carcinoma of the lung, as described (36), and cultured in DMEM/F12 1:1 medium containing 10% heat-inactivated FCS, 1% Ultroser G (Gibco BRL, Life Technologies, Cergy Pontoise, France). The Heu161 CTL clone was isolated from autologous tumor-infiltrating lymphocytes, as described (18). The resistant cell line to CTL lysis, IGR-HeuR, was derived from IGR-Heu and was established after 3 months of coculture with the autologous CTL. The cell line was then cloned by limiting dilution, and several clones, including IGR-HeuR8, were isolated.

Analysis of MHC Class I, Transporter-Associated with Antigen Processing (TAP), and Endoplasmic Reticulum Amino Peptidase (ERAP) Expression. ERAPI, MHC Class I and TAP-1 were analyzed by immunoprecipitation followed by immunoblotting. Each cell type was lysed in 50 mM Tris/150 mM NaCl/1% Triton X-100, pH 7.9, for 30 min. The supernatant was precleared with Sepharose beads coupled with a nonspecific mouse mAb for 3 h at 4°C. Equal amounts of the supernatant were incubated for 1 h at 4°C with mAb precoupled to Sepharose beads specific for MHC Class I (W6/32) and ERAP1 (4D2) (37). Anti-TAP-1 mAb (148.3) (38) was also incubated with an equal amount of supernatant for 1 h and was immunoprecipitated with protein G beads for 30 min after incubation with antibody. ERAP1 was detected with mAb 6H9, MHC class I detected with a rabbit polyclonal antibody (R5996-4, kindly provided by N. Tanigaki, Roswell Park Cancer Institute, Buffalo, NY), and TAP-1 was detected with mAb 148.3. ERAP2 and proteasome expression was analyzed in complete cell lysates. Proteasome was detected by using mAb MCP21 (kindly provided by G. Niedermann, University Hospital for Radiology, Freiburg, Germany). ERAP2 was detected by using mAb 3F5 (37).

Cytolytic Activity Assay. The cytotoxic activity of the CTL clone was measured by a conventional 4-h ^{51}Cr-release assay by using triplicate cultures in round-bottomed 96-well plates. Effector/target ratios were 30:1, 15:1, 5:1, and 1:1 on 2,000 target cells per well. Percent specific cytotoxicity was calculated conventionally.

Confocal Microscopy. For actin staining, tumor cells and autologous CTL were mixed in a 1:2 target/effector ratio and then

plated on poly(L-lysine)-coated coverslips, fixed with 3% formaldehyde/PBS for 10 min, and permeabilized with 0.1% Triton X-100/PBS for 5 min, followed by blocking with 1% BSA/PBS for 20 min. The fixed cells were stained with Alexa Fluor 568-phalloidin (Molecular Probes). Nucleus was stained with TO-Pro 3 (Molecular Probes). The stained cells were analyzed by using a fluorescence microscope (Zeiss).

Electron Microscopy. CTLs and tumor cells on coverslips were fixed with 2.5% glutaraldehyde in 0.1 M cacodylate buffer, pH 7.4. Cells were postfixed with 2% OsO_4 for 45 min on ice, dehydrated in increasing concentrations of ethanol, and embedded in Epon while on coverslips. Ultrathin sections were prepared with a Reichert UltracutS ultramicrotome (Leica, Vienna), and viewed with a TEM CM120 Philips electron microscope (FEI, Eindhoven, The Netherlands) after counterstaining with uranyl acetate.

TaqMan Real-Time Quantitative Reverse Transcription-PCR Analysis. For analysis of granzyme B and perforin induction, T cells were conjugated with tumor cells at a 1:1 ratio during 30 min, 2 h, 4 h, and 6 h. RNA extraction was performed with TRIzol reagent and followed by Taqman for *granzyme B* and *perforin* genes. PCR primers and probe for the gene target were designed by Applied Biosystems and used according to the manufacturer's recommendations. The amount of sample RNA was normalized by the amplification of an endogenous control (18S). The relative quantification of the transcripts was derived by using the standard curve method (Applied Biosystems User Bulletin 2, ABI PRISM 7700 Sequence Detection System).

Oligo Microarray Technology. Sensitive and resistant cell line total RNA were directly compared by using Agilent oligonucleotide dual-color technology, running dye swap and duplicate experiments. Probe synthesis and labeling were performed by Agilent's Low Fluorescent Low input Linear Amplification Kit. Hybridization was performed on human whole-genome 44,000 oligonucleotide microarrays (Agilent, Palo Alto, CA) by using reagents and protocols provided by the manufacturer. Feature extraction software provided by Agilent (Version 7.5) was used to quantify the intensity of fluorescent images and to normalize results using the linear and lowess subtraction method. Primary analysis was performed by using RESOLVER software (Rosetta Laboratories, Milan) to identify genes differentially expressed between resistant and sensitive cell lines (IGR-Heu/IGR HeuR8) with a fold change >2 and P value $<10^{-10}$.

RNA Interference. Gene silencing of *scinderin* and *ephrin-A1* expression was performed by using sequence-specific siRNA, purchased from Proligo (Boulder, CO). Briefly, cells were transfected by electroporation with 50 nM siRNA in a Gene Pulser Xcell Electroporation System (Bio-Rad; 300 V, 500 μF) and then allowed to grow for 72 h. Human *ephrin-A1* and *scinderin* siRNA sequences were 5′-GACACCAAUUGUCAUCAUAAA-3′ and 5′-GACACAGCUACUACUACAUCU-3′. A siRNA targeting EGFP was used as a negative control 5′-GCAAGCUGACCCUGAAGUUCAU-3′ (39). All sequences were evaluated for gene specificity by using the National Institutes of Health BLAST program.

We thank G. Trinchieri and F. Marincola for discussion and critical reading of the manuscript. We thank V. Lazar and P. Dessen for microarray analysis, C. Leroy for secretarial assistance, and Y. Lecluse for FACS analysis. This work was supported by grants from La Ligue Nationale Contre le Cancer and the Association Contre le Cancer (3501-3354).

1. Schreiber, K. L. & Forman, J. (1990) *J. Immunol.* **144,** 2018–2026.
2. Boon, T., Cerottini, J. C., Van den Eynde, B., van der Bruggen, P. & Van Pel, A. (1994) *Annu. Rev. Immunol.* **12,** 337–365.
3. Chouaib, S., Asselin-Paturel, C., Mami-Chouaib, F., Caignard, A. & Blay, J. Y. (1997) *Immunol. Today* **18,** 493–497.
4. Dunn, G. P., Bruce, A. T., Ikeda, H., Old, L. J. & Schreiber, R. D. (2002) *Nat. Immunol.* **3,** 991–998.
5. Dunn, G. P., Old, L. J. & Schreiber, R. D. (2004) *Immunity* **21,** 137–148.
6. Khong, H. T. & Restifo, N. P. (2002) *Nat. Immunol.* **3,** 999–1005.
7. De Bono, J. S., Tolcher, A. W. & Rowinsky, E. K. (2003) *Breast Cancer Res.* **5,** 154–159.
8. Rimsza, L. M., Roberts, R. A., Miller, T. P., Unger, J. M., LeBlanc, M., Braziel, R. M., Weisenberger, D. D., Chan, W. C., Muller-Hermelink, H. K., Jaffe, E. S., *et al.* (2004) *Blood* **103,** 4251–4258.
9. Huang, B., Zhao, J., Li, H., He, K. L., Chen, Y., Mayer, L., Unkeless, J. C. & Xiong, H. (2005) *Cancer Res.* **65,** 5009–5014.
10. Bots, M., Kolfschoten, I. G., Bres, S. A., Rademaker, M. T., de Roo, G. M., Kruse, M., Franken, K. L., Hahne, M., Froelich, C. J., Melief, C. J., *et al.* (2005) *Blood* **105,** 1153–1161.
11. Janke, J., Schluter, K., Jandrig, B., Theile, M., Kolble, K., Arnold, W., Grinstein, E., Schwartz, A., Estevez-Schwarz, L., Schlag, P. M., *et al.* (2000) *J. Exp. Med.* **191,** 1675–1686.
12. Gajate, C. & Mollinedo, F. (2005) *J. Biol. Chem.* **280,** 11641–11647.
13. Rosen, K., Rak, J., Leung, T., Dean, N. M., Kerbel, R. S. & Filmus, J. (2000) *J. Cell Biol.* **149,** 447–456.
14. Watzl, C. & Long, E. O. (2003) *J. Exp. Med.* **197,** 77–85.
15. Sechi, A. S. & Wehland, J. (2004) *Trends Immunol.* **25,** 257–265.
16. Barda-Saad, M., Braiman, A., Titerence, R., Bunnell, S. C., Barr, V. A. & Samelson, L. E. (2005) *Nat. Immunol.* **6,** 80–89.
17. Hall, A. (1998) *Science* **279,** 509–514.
18. Echchakir, H., Vergnon, I., Dorothee, G., Grunenwald, D., Chouaib, S. & Mami-Chouaib, F. (2000) *Int. Immunol.* **12,** 537–546.
19. Thiery, J., Abouzahr, S., Dorothee, G., Jalil, A., Richon, C., Vergnon, I., Mami-Chouaib, F. & Chouaib, S. (2005) *J. Immunol.* **174,** 871–878.
20. Spector, I., Shochet, N. R., Kashman, Y. & Groweiss, A. (1983) *Science* **219,** 493–495.
21. Rodriguez Del Castillo, A., Lemaire, S., Tchakarov, L., Jeyapragasan, M., Doucet, J. P., Vitale, M. L. & Trifaro, J. M. (1990) *EMBO J.* **9,** 43–52.
22. Beckmann, M. P., Cerretti, D. P., Baum, P., Vanden Bos, T., James, L., Farrah, T., Kozlosky, C., Hollingsworth, T., Shilling, H., Maraskovsky, E., *et al.* (1994) *EMBO J.* **13,** 3757–3762.
23. Kwiatkowski, D. J. (1999) *Curr. Opin. Cell Biol.* **11,** 103–108.
24. Iida, H., Honda, M., Kawai, H. F., Yamashita, T., Shirota, Y., Wang, B. C., Miao, H. & Kaneko, S. (2005) *Gut.* **54,** 843–851.
25. Potla, L., Boghaert, E. R., Armellino, D., Frost, P. & Damle, N. K. (2002) *Cancer Lett.* **175,** 187–195.
26. Liu, K., Caldwell, S. A. & Abrams, S. I. (2005) *Cancer Res.* **65,** 4376–4388.
27. Shankaran, V., Ikeda, H., Bruce, A. T., White, J. M., Swanson, P. E., Old, L. J. & Schreiber, R. D. (2001) *Nature* **410,** 1107–1111.
28. Kutsuna, H., Suzuki, K., Kamata, N., Kato, T., Hato, F., Mizuno, K., Kobayashi, H., Ishii, M. & Kitagawa, S. (2004) *Am. J. Physiol.* **286,** C55–C64.
29. Zhou, G., Lu, Z., McCadden, J. D., Levitsky, H. I. & Marson, A. L. (2004) *J. Exp. Med.* **200,** 1581–1592.
30. So, T., Takenoyama, M., Mizukami, M., Ichiki, Y., Sugaya, M., Hanagiri, T., Sugio, K. & Yasumoto, K. (2005) *Cancer Res.* **65,** 5945–5952.
31. Nowak, D., Skwarek-Maruszewska, A., Zemanek-Zboch, M. & Malicka-Blaszkiewicz, M. (2005) *Acta. Biochim. Pol.* **52,** 461–468.
32. Miyamoto, S., Akiyama, S. K. & Yamada, K. M. (1995) *Science* **267,** 883–885.
33. Mills, J. C., Stone, N. L. & Pittman, R. N. (1999) *J. Cell Biol.* **146,** 703–708.
34. Dodelet, V. C. & Pasquale, E. B. (2000) *Oncogene* **19,** 5614–5619.
35. Carter, N., Nakamoto, T., Hirai, H. & Hunter, T. (2002) *Nat. Cell Biol.* **4,** 565–573.
36. Asselin-Paturel, C., Echchakir, H., Carayol, G., Gay, F., Opolon, P., Grunenwald, D., Chouaib, S. & Mami-Chouaib, F. (1998) *Int. J. Cancer* **77,** 7–12.
37. Saveanu, L., Carroll, O., Lindo, V., Del Val, M., Lopez, D., Lepelletier, Y., Greer, F., Schomburg, L., Fruci, D., Niedermann, G., *et al.* (2005) *Nat. Immunol.* **6,** 689–697.
38. Meyer, T. H., van Endert, P. M., Uebel, S., Ehring, B. & Tampe, R. (1994) *FEBS Lett.* **351,** 443–447.
39. Caplen, N. J., Parrish, S., Imani, F., Fire, A. & Morgan, R. A. (2001) *Proc. Natl. Acad. Sci. USA* **98,** 9742–9747.